SCCWRP #0608

SETAC PRESS

Environmental Toxicology and Chemistry, Vol. 29, No. 2, pp. 265–274, 2010
© 2009 SETAC
Printed in the USA
DOI: 10.1002/etc.54

EXCHANGE OF POLYCYCLIC AROMATIC HYDROCARBONS AMONG THE ATMOSPHERE, WATER, AND SEDIMENT IN COASTAL EMBAYMENTS OF SOUTHERN CALIFORNIA, USA

Lisa D. Sabin,*† Keith A. Maruya,† Wenjian Lao,† Dario Diehl,† David Tsukada,† Keith D. Stolzenbach,‡ and Kenneth C. Schiff†

†Southern California Coastal Water Research Project, 3535 Harbor Boulevard, Suite 110, Costa Mesa, California 92626, USA

‡Department of Civil and Environmental Engineering, 5732J Boelter Hall, University of California, Los Angeles, California 90095-1593, USA

(*Submitted* 16 *April* 2009; *Returned for Revision* 2 *June* 2009; *Accepted* 2 *September* 2009)

Abstract—The present study investigated cross-media transport between both the sediment and the water column and between the water column and the atmosphere, to understand the role of each compartment as a source or a sink of polycyclic aromatic hydrocarbons (PAH) in southern California, USA, coastal waters. Concentrations of PAH were measured in the atmosphere, water column, and sediment at four water-quality-impaired sites in southern California: Ballona Creek Estuary, Los Angeles Harbor, Upper Newport Bay, and San Diego Bay. These concentrations were used to calculate site-specific sediment–water and atmosphere–water exchange fluxes. The net sediment–water exchange of total PAH (*t*-PAH) was positive, indicating that sediments were a source to the overlying water column. Furthermore, the net atmosphere–water exchange (gas exchange + dry particle deposition) of *t*-PAH was typically positive also, indicating the water column was a net source of PAH to the surrounding atmosphere through gas exchange. However, in all cases, the magnitude of the diffusive flux of PAH out of the sediments and into the water column far exceeded input or output of PAH through air/water exchange processes. These results demonstrate the potential importance of contaminated sediments as a source of PAH to the water column in coastal waters of southern California. Environ. Toxicol. Chem. 2010;29:265–274. © 2009 SETAC

Keywords—Atmospheric deposition Sediment flux Polycyclic aromatic hydrocarbon

INTRODUCTION

Polycyclic aromatic hydrocarbons (PAH) are directly emitted into the atmosphere and discharged into water bodies and may accumulate in coastal estuarine and marine sediments [1–3]. Anthropogenic sources of PAH in the atmosphere are primarily from fossil fuel combustion (e.g., gasoline and diesel vehicle exhaust, power plant, and industrial emissions). Anthropogenic sources to the water and sediment include atmospheric deposition, direct discharges of petroleum products from shipping activities to coastal waters, industrial and wastewater sources, and urban stormwater runoff [4–7]. Managing PAH levels in contaminated water bodies requires understanding of the transport among the atmosphere, water column, and bottom sediments.

In other regions, a number of studies have investigated the role of the atmosphere as a potential source of PAH to polluted water bodies, especially near urban centers [8–12]. Significant research has been conducted on the accumulation of PAH in sediments, partitioning between the sediment and porewater and exchange between the overlying water and contaminated bottom sediments [5,13–22]. However, few studies offer synoptic measurements to calculate both the air–water and the sediment–water exchange fluxes for a given water body. Furthermore, no studies have been conducted on atmospheric deposition of PAH in the coastal waters of southern California, USA.

The Southern California Bight (SCB) is located adjacent to the second most populous region in the United States, including the cities of Los Angeles and San Diego. This region has some of the worst air quality in the nation, with high atmospheric concentrations of PAH. Furthermore, coastal urban embayments within the SCB are enriched in PAH relative to nearshore coastal waters [1]. A recent survey of sediments in the SCB found more than 70% of the SCB area was contaminated with anthropogenic organic compounds, including PAH, and the highest concentrations were associated with bays, harbors, and estuaries [23]. In contrast to the legacy organochlorines (e.g., DDT and polychlorinated biphenyl), which have been banned from production and use for nearly three decades, PAH continue to be introduced into the southern California environment via multiple sources.

The goal of the present study was to examine the potential importance of different environmental compartments as sources or sinks of PAH in the SCB. The objectives were to characterize the distribution of PAH in the atmosphere, the water column, and the sediment and to quantify the magnitude and direction of exchange among these compartments in selected bays, harbors, and estuaries of the SCB.

MATERIALS AND METHODS

Concentrations of PAH were measured in the atmosphere (gas and particle phase), the water column (dissolved and sorbed to suspended particulate matter [SPM]), and the surface sediment, along with measurements of total suspended solids (TSS) and total organic carbon at four sites in the SCB. From these measurements, fluxes between compartments were

* To whom correspondence may be addressed (lisas@sccwrp.org).

Published online 4 November 2009 in Wiley InterScience (www.interscience.wiley.com).

estimated, including gas exchange between the atmosphere and the water column, dry deposition of particles from the atmosphere to the water surface, sedimentation of SPM in the water column to the bottom sediment, and diffusive flux between sediment pore water and the water column. Gas exchange was estimated based on a modified two-film transfer model with inputs of wind speed and Henry's Law constants. For sediment–water exchange, pore-water concentrations were estimated from measured sediment concentrations and the organic-carbon normalized partition coefficient. A simple diffusive flux model based on concentration gradients between pore water and the water column was used to calculate the exchange flux. Dry deposition and sedimentation fluxes were estimated from measured concentrations and assumed deposition and sedimentation velocities, respectively.

Sample collection

Four coastal estuaries within the SCB were sampled for PAH during the summer and fall of 2006 (Fig. 1). All study sites were located near urban areas with varying degrees of local contaminant sources and historical sources of PAH, and all sites are listed as impaired on the State of California 303(d) list because of elevated levels of PAH in fish tissue, sediment, and/or the water column [24]. The Ballona Creek Estuary (BCE) site, adjacent to Santa Monica Bay, is primarily urbanized, with no permitted wastewater or industrial discharges. The Los Angeles Harbor (LAH) site, adjacent to a heavily urbanized area, is the largest commercial port in the United States. The Upper Newport Bay (UNB) site is the largest coastal wetland in southern California and drains a watershed that is primarily residential/commercial [7]. The San Diego Bay (SDB) site is home to one of the largest naval facilities in the United States and is also adjacent to a large urban area.

All air samples were collected at land-based sites selected to be generally representative of PAH sources near the target water bodies, and not influenced by other sources not present at the water bodies themselves. Air samples for BCE were collected on a rooftop approximately 4 km directly south of the estuary, at a coastal site upwind of urban PAH sources. Similarly to the estuary, this location was influenced predominantly by onshore flow of marine air. Air samples for the LAH site were collected at an existing South Coast Air Quality Management District (SCAQMD) site located 3 km directly downwind of the inner harbor. The PAH sources near this site were predominantly the same as those at the Inner Harbor where the water/sediment samples were collected, which was located in the Consolidated Slip shipping basin, near the mouth of Dominguez Channel. Air samples for the UNB site were collected inside the University of California, Irvine, Marsh Reserve, located 2 km directly downwind of the water/sediment collection site inside the bay, near

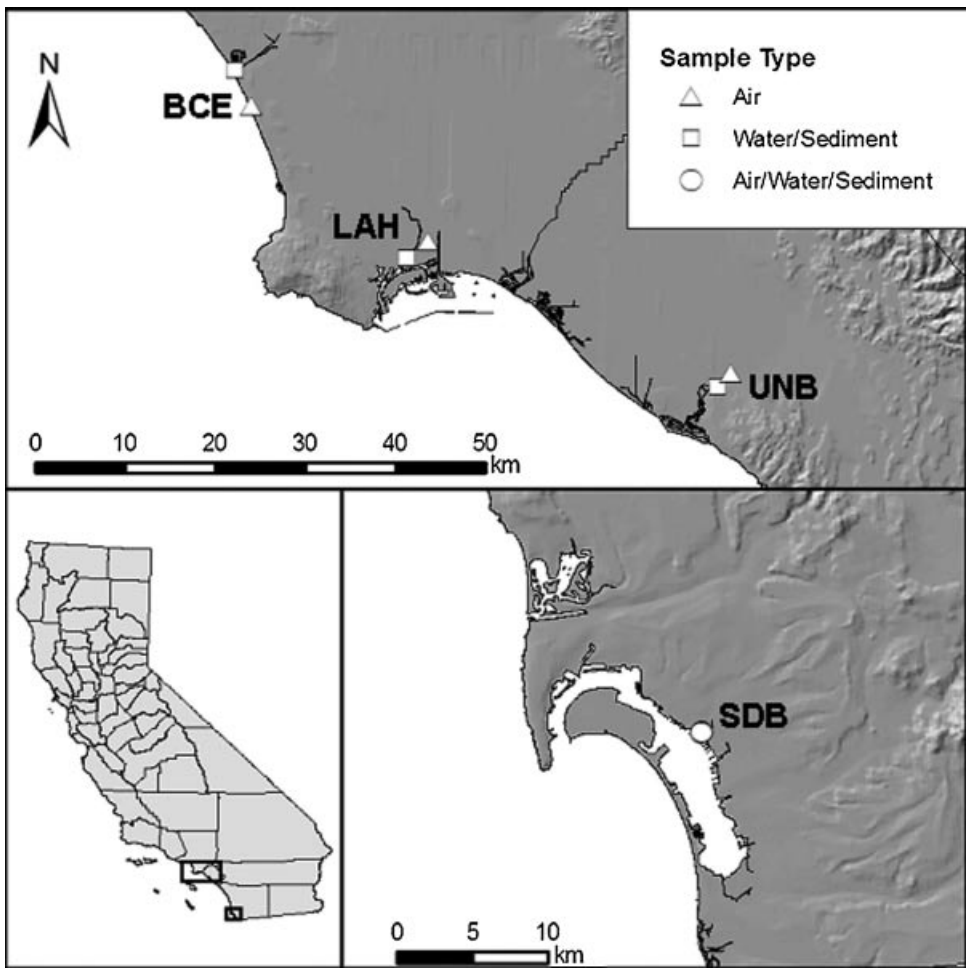

Fig. 1. Map of sample collection sites (CA, USA) for air, water, and sediment. BCE, Ballona Creek Estuary; LAH, Los Angeles Harbor; UNB, Upper Newport Bay; SDB, San Diego Bay.

Table 1. Site specific sampling information[a]

Site	Matrix	No. samples collected	Collection date(s) (2006)	Air temperature (°C)	Wind speed (m/s)	Total suspended solids (mg/L)	Sediment total organic carbon
Ballona Creek Estuary, CA, USA	Air	1	Oct 31–2 Nov	20 ± 4	3.4 ± 0.8		
	Water	1	Aug 6			4.9	
	Sediment	3	Jul 13				1.1%
			Jul 25				
			Sep 25				
Los Angeles Harbor, CA, USA	Air	3	Sept 19–21	20 ± 2	2.0 ± 0.5		
			Oct 18–20				
			Oct 24–26				
	Water	3	Sept 11–18			5.1 ± 1.7	
			Sept 22–25				
			Nov 13–18				
	Sediment	4	Sep 18				5.6% ± 0.3%
			Sep 14				
			Sep 22				
			Oct 22				
Upper Newport Bay, CA, USA	Air	1	Aug 16–18	24 ± 4	2.2 ± 0.3		
	Water	1	Jul 22			18	
	Sediment	4	Jul 22				1.3%
San Diego Bay, CA, USA	Air	1	Sept 27–29	21 ± 1	2.8 ± 0.6		
	Water	2	Sept 15–18			1.1 ± 0.7	
			Sept 27–Oct 1				
	Sediment	2	Sep 15				2.91%

[a] Mean ± standard deviation for temperature, wind speed, total suspended solids, and sediment total organic carbon.

the mouth of San Diego Creek. Air samples for the SDB site were collected from the roof of the San Diego Naval Station, adjacent to the bay, approximately 30 m from where the water/sediment samples were collected inside the bay at the mouth of Chollas Creek.

Each site was sampled at least once in each compartment (air, water, and sediment; Table 1). Daily meteorological data (temperature and wind speed) were obtained from nearby National Weather Service stations (Los Angeles International Airport, Long Beach Airport, John Wayne Airport, and San Diego Lindbergh Field for BCE, LAH, UNB, and SDB, respectively; National Climatic Data Center [NCDC], 2006; http://www.ncdc.noaa.gov/oa.ncdc.html).

Air samples were collected using a high-volume sampler (Anderson Instruments) equipped with a quartz fiber filter (QFF; Whatman; 0.7-μm pore size) to collect particle-phase compounds, followed by a polyurethane foam (PUF) plug (7 cm long and 6 cm in diameter) held in a glass sleeve to collect gas-phase compounds. The gas phase was operationally defined as the concentration retained on the PUF. A sample flow rate of 0.25 m^3/min was used over a period of 24 to 48 h. Prior to sampling, QFFs were wrapped in aluminum foil and baked at 425°C for 6 h, then stored in hexane-rinsed aluminum-foil-lined Petri dishes. Polyurethane foam plugs were cleaned by extraction with pesticide-grade acetone for 24 h, followed by extraction using 10% diethyl ether/90% *n*-hexane mixture for 4 h, dried, then stored in precleaned glass jars with hexane-rinsed, aluminum-foil-lined lids. After sampling, the QFFs and PUFs were returned to their original jars, wrapped in aluminum foil, transported to the laboratory in an ice chest, and stored at 4°C.

Water column samples for the dissolved phase, operationally defined as filtrates passing through a 0.7-μm glass fiber filter (GFF), and the particle phase were collected with an Infiltrex 100 in situ water pumping system (Axys Environmental Systems), described in detail previously [25]. Briefly, water is continuously pumped through a stack of eight GFFs (Whatman; 0.7-μm pore size) to retain particles and a polytetrafluoroethylene (PTFE) column packed with XAD-II resin (Supelco) to extract dissolved organics. The pump was positioned in the water column 1 m above the sediment–water interface. The unit was anchored on the seafloor by two iron chain links and suspended in the water column with a subsurface float. The pump flow rate was set at 200 to 400 ml/min. After sampling, the PTFE column was processed within 24 h, and GFFs were stored at −20°C.

Discrete water samples were collected with 5-L Niskin bottles for determination of TSS. Discrete samples were immediately sealed in containers with Teflon®-lined lids and transported to the laboratory on ice, then stored at 4°C.

Surface sediment (top 5 cm) was collected with either a stainless-steel modified Van Veen or petite Ponar grab and transferred into precleaned 500-ml glass jars. One grab per site was collected on each day of sampling. The sediment samples were placed on ice for transport and then stored in the laboratory at −20°C.

Analytical procedures

In total, 28 individual PAH with two to six rings were targeted in the present study (Table 2). Total PAH (*t*-PAH) was defined as the sum of these 28 compounds.

All laboratory glassware was washed with soap and water, rinsed with deionized water, and kilned at approximately 500°C for at least 4 h. Sediment samples were freeze-dried before extraction. The PTFE columns with XAD-II resin were eluted with dichloromethane (DCM). The glass fiber filters and QFFs were extracted with DCM using an ASE300 accelerated solvent extraction system (Dionex). Extraction conditions were as follows: 100°C, 1,500 psi, stationary time 5 min, flushing volume 60%. Three extraction cycles were carried out for each sample. The PUF samples were Soxhlet extracted with

Table 2. Target polycyclic aromatic hydrocarbon compounds

Name	Abbreviation
Naphthalene	N
1-Methylnaphthalene	1MeN
2-Methylnaphthalene	2MeN
Acenaphthylene	Acey
Acenaphthene	Ace
Biphenyl	BP
2,6-Dimethylnaphthalene	DMN
Fluorene	Flu
2,3,5-Trimethylnaphthalene	TMN
Anthracene	An
Phenanthrene	Ph
1-Methylphenanthrene	1MePh
2-Methylphenanthrene	2MePh
Fluoranthene	Fla
Pyrene	Py
3,6-Dimethylphenanthrene	DMPh
11H-Benzo[*b*]fluorene	B*b*Flu
Benz[*a*]anthracene	B*a*A
Chrysene + triphenylene	Chry
Benzo[*a*]pyrene	B*a*P
Benzo[*b* + *j*]fluoranthene	B*b*F
Benzo[*e*]pyrene	B*e*P
Benzo[*k*]fluoranthene	B*k*F
Perylene	Peryl
Benzo[*ghi*]perylene	B*ghi*P
Indeno[1,2,3-*cd*]pyrene	I123*cd*P
Dibenz[*a,h*/*a,c*]anthracene	DB*a,h*A
9,10-Diphenylanthracene	DP*h*A

n-hexane/ethyl ether (9:1, v/v) for 18 h. Freeze-dried sediments were Soxhlet extracted with DCM for 18 h. Sample extracts were concentrated, and the solvent was exchanged to hexane. The extract was kept in the dark overnight at room temperature after a small amount of activated copper had been added to remove sulfur.

Cleanup of all sample extracts was performed using silica gel/alumina column chromatography. The two sorbents were pre-extracted three times with DCM using the ASE300 system, dried, and activated overnight at 180 and 250°C, respectively. Silica gel and alumina were subsequently deactivated by using 3% (w/w) double-deionized water. After the sample extract had been loaded, the first 20 ml of hexane eluent and the subsequent 70 ml of 30:70% DCM/hexane mixture were collected. Sample extracts were concentrated to <5 ml using a vacuum rotary evaporator and further reduced to 500 μl using a gentle stream of ultrahigh-purity (>99.999%) nitrogen.

Total suspended solid was measured by filtering a 25- to 3,000-ml aliquot of sample through a tared GFF (Whatman, 25 mm diameter, 0.7 μm pore size). After being dried in an oven at 60°C for 24 h, the loaded filter was weighed to the nearest 0.001 g. The mass of inorganic salt residues was subtracted from all TSS mass determinations. For total organic carbon in sediment, an aliquot of each dried sample was acidified with hydrochloric acid vapors to remove inorganic carbon. The acidified sample was then dried, packed in a tin boat, and analyzed using a Carlo Erba 1108 CHN elemental analyzer (Thermo Fisher Scientific) equipped with an AS/23 autosampler.

Sample extracts containing target PAH were analyzed by Varian 3800 gas chromatography (GC)/Saturn 2000 ion trap mass spectrometry (MS) systems (Varian). A splitless volume of 1 μl was injected at 100°C. After holding for 0.05 min, the injector temperature was increased to 280°C at approximately 200°C/min and held for 20 min. Carrier gas was helium (>99.999%) at a flow rate of 1.0 ml/min. Chromatographic separations were made with a 60 m × 0.25 mm inner diameter (0.25 μm film thickness) DB-5MS column (J&W Scientific/Agilent) programmed from 80°C (1 min hold) to 176°C at 8°C/min, followed by a ramp to 230°C at 1.5°C/min, and a final increase to 290°C at 5°C/min (39 min hold). Selected ion storage mode was used to analyze the samples. Quantification of individual analyte concentrations was by the internal standard method (2-fluorobiphenyl, *p*-terphenyl-d_{14}, dibenzo[*a,h*]anthracene-d_{14} as the internal standards) using a six-point (50–2,000 ppb) calibration curve. Extracts were diluted and/or concentrated accordingly to bring analyte concentrations into the calibration range.

Quality assurance

For atmospheric samples, field blanks consisting of precleaned QFFs and PUFs, transported to and from the field for each sampling event, were handled and processed in the same manner as samples. On average, these field blanks were 8 and 22% of samples for QFFs and PUFs, respectively, and concentrations in the corresponding atmospheric samples were field blank corrected. No PAH was detected on procedural blanks for any of the other media, which were analyzed using the same protocols followed for analysis of samples.

Because sample volumes, particularly for the water column, were variable, detection limits were sample and compound specific. Detection limits in the atmosphere ranged from 1.5 to 86 pg/m^3 in the gas phase and from 0.15 to 8.8 ng/g in the particle phase. In the water column, detection limits ranged from 0.010 to 0.60 ng/L in the dissolved phase and from 0.15 to 8.8 ng/g dry weight on SPM. Sediment detection limits ranged from 0.4 to 24 ng/g dry weight. Samples were spiked with a mixture of surrogates (naphthalene-d_8, acenaphthylene-d_{10}, phenanthrene-d_{10}, chrysene-d_{12}, perylene-d_{12}, benzo[*ghi*]perylene-d_{12}) prior to extraction to estimate recovery efficiency. Standard reference materials (e.g., SRM1941b: a marine sediment) were extracted and analyzed following the same procedures as the samples. Mean recoveries (±standard deviation) were 86% ± 20% (atmosphere-gas phase), 77% ± 15% (atmosphere-particle phase), 85% ± 6% (water column-dissolved), 93% ± 24% (water column-SPM), and 94% ± 13% (sediment, SRM1941b). Because mean recoveries were considered quantitative (>70%), sample concentrations were not corrected for surrogate recovery.

Data analysis

Air–water exchange calculations focused on gas exchange at the air–water interface and dry particle deposition from the atmosphere to the water. Sediment–water exchange calculations included diffusive transport between the sediment pore water and the overlying water column and sedimentation of SPM from the water column. For each exchange process, a flux was calculated for individual PAH compounds and summed to give a total.

For concentration sums and flux calculations, one-half method detection limit was substituted for concentrations below the detection limit. If a compound was below detection in both

air and water for gas exchange, or both water and sediment for diffusive sediment–water exchange, no flux calculation was made.

Gas exchange model

Calculations of gas exchange between the atmosphere and the water were based on a modified two-film resistance model [26,27]. In this model, the rate of transfer is controlled by diffusion across the air–water interface. The net flux is defined by

$$F = k_{ol}\,(C_w - C_a/H') \quad (1)$$

where F is the net flux (ng/m^2/day), k_{ol} is the overall mass transfer coefficient (m/day), C_w and C_a are the dissolved and gaseous phase concentrations (ng/m^3) in water and air, respectively, and H' is the dimensionless Henry's Law constant. The reciprocal of k_{ol} is the sum of the resistance to mass transfer in the air and water, as

$$1/k_{ol} = 1/k_w + 1/(k_a \cdot H') \quad (2)$$

where k_w and k_a are the water-side and air-side mass transfer coefficients, respectively. The following correlation was used to calculate k_a for H_2O vapor [28]:

$$k_{a(H_2O)} \approx 0.2 \cdot u_{10} + 0.3 \quad (3)$$

where $k_{a(H_2O)}$ is the mass transfer coefficient in air for H_2O (cm/s), and u_{10} is the wind speed (m/s) above the water surface at 10 m.

The following equation was used to calculate k_w for CO_2 [29]:

$$k_{w(CO_2)} = 0.45 \cdot {u_{10}}^{1.64} \quad (4)$$

where $k_{w(CO_2)}$ is the mass transfer coefficient in water for CO_2. The relationships in Equations 3 and 4 have been used previously by a number of researchers to calculate gas exchange of organic compounds over water [30–32].

Because the rate of transfer is related to the molecular diffusivity, these estimates for $k_{a(H_2O)}$ and $k_{w(CO_2)}$ allow prediction of k_a and k_w for other compounds of interest with the following relationships [28]:

$$k_{a(unknown)} = k_{a(H_2O)} \cdot [D_{a(unknown)}/D_{a(H_2O)}]^{0.67} \quad (5)$$

where D_a is the molecular diffusivity in air, and

$$k_{w(unknown)} = k_{w(CO_2)} \cdot [Sc_{(unknown)}/Sc_{(CO_2)}]^{-1/2} \quad (6)$$

where Sc is the Schmidt number, calculated by dividing the kinematic viscosity of seawater at 20°C (cm^2/s) by the molecular diffusivity in water (D_w).

Mean air and water concentrations and mean wind speeds from each site were used in the above equations to calculate the net gas exchange flux at each site. Other inputs included the temperature-dependent molecular diffusivities of individual compounds in air (D_a) and water (D_w) and temperature-dependent Henry's Law constants. The D_a and D_w for 20°C were calculated based on the method of Fuller et al. [33] and Wilke and Chang [34], respectively, employing the LeBas molar volume estimates as needed. Temperature-corrected Henry's Law constants for 20°C were obtained from Bamford et al. [35], when reported, or otherwise from compiled chemical properties [36].

Dry particle deposition model

Dry particle deposition was calculated from measured particle concentrations in the air and the particle deposition velocity:

$$F = C_p \cdot V_d \quad (7)$$

where F is the dry deposition flux (ng/m^2/d), C_p (ng/m^3) is the particle-phase concentration of the compound in the air, and V_d (cm/s) is the dry deposition velocity of the particles in the air. A deposition velocity of 0.2 cm/s was used for the present study, as recommended by the Integrated Atmospheric Deposition Network [8].

Diffusive flux model

The model of diffusive exchange between the water column and the sediment was based on Fick's gradient-flux law, assuming a well-mixed upper sediment layer (top 5 cm) and equilibrium between the sediment and the porewater up to the boundary layer. The flux across the sediment–water interface was calculated as follows:

$$F = k_s\,(C_{pw} - C_w) \quad (8)$$

where F is the diffusive flux between the sediment and the water column (ng/m^2/day); C_w and C_{pw} are the water column and porewater concentrations (ng/m^3), respectively; and k_s (m/day) is the sediment–water mass transfer coefficient. Compound specific k_s values were calculated as follows [28]:

$$k_s = D_w/h \quad (9)$$

where D_w (m^2/day) is the temperature-dependent molecular diffusion coefficient and h (m) is the thickness of the boundary layer. A typical value for h of 5×10^{-4} m was used [28].

Sediment pore-water concentrations were calculated from sediment concentrations as follows:

$$C_{pw} = C_{sed}/(K_{OC} \cdot f_{OC}) \quad (10)$$

where C_{pw} (ng/m^3) is the concentration in the pore water, C_{sed} (ng/g) is the concentration in the sediment, K_{OC} (ml/g) is the organic carbon normalized partition coefficient, and f_{OC} is the fraction of organic carbon in the sediment. The K_{OC} values were obtained from compiled chemical properties [37,38]. The average value for sediments was used when available.

Sedimentation model

Sedimentation of organic compounds sorbed to SPM in the water column was calculated analogously to the dry particle deposition flux:

$$F = W_s \cdot C_s \quad (11)$$

where C_s (ng/m^3) is the sorbed concentration of organic compound on SPM in the water column and W_s (m/day) is the sedimentation velocity. A value of 1 m/day was used for W_s [39].

RESULTS AND DISCUSSION

Sampling conditions and multimedia concentrations

Daily average wind speeds during atmospheric sampling at the four sites ranged from 2.0 to 3.4 m/s, and daily average temperatures ranged from 20 to 24°C (Table 1). Mean TSS in the water column ranged from 1.1 to 18 mg/L, and sediment organic carbon ranged from 1.1 to 5.6% (Table 1). Detectable concentrations of PAHs were found in air, water, and sediment at all sites (Table 3).

Atmospheric concentrations of *t*-PAH (gas + particle) ranged from 3.6 to 28 ng/m^3. The gas phase accounted for 90% of the total atmospheric concentrations at all sites. The majority of the particle phase was made up of of four- to six-ring PAH (56–83%), whereas the gas phase was dominated by two- or three-ring PAH (55–73%), except at SDB (45%). Concentrations of individual PAH ranged from not detected (ND) to 11 ng/m^3 in the gas phase and from ND to 0.68 ng/m^3 in the particle phase. The largest contributors to *t*-PAH (gas + particle) were phenanthrenes (parent and methylated), fluoranthene, and pyrene (73–96%).

Water column concentrations of *t*-PAH ranged from 5.6 to 74 ng/L in the dissolved phase and from 3.3 to 72 ng/L on SPM. Concentrations of individual PAH ranged from ND to 22 ng/L in the dissolved phase and from ND to 17 ng/L on SPM. As in the atmosphere, phenanthrenes (parent and methylated), fluoranthene, and pyrene dominated water concentrations, contributing between 57 and 70% in the dissolved phase and between 48 and 78% in the sorbed phase. Most of the remaining PAH on SPM was contributed by other four- to six-ring PAH compounds (e.g., benzo[*b* + *j*]fluoranthene, chrysene, etc.).

Concentrations of *t*-PAH in the sediment ranged from 657 to 11,000 ng/g dry weight. Four- to six-ring compounds dominated (85–91%). Individual PAH concentrations in the sediment ranged from ND to 1,600 ng/g dry weight. Typically, the largest contributions were from fluoranthene (10–12%), pyrene (11–18%), and chrysene (12–15% at all sites except UNB).

For all media, concentrations generally followed the pattern of highest to lowest as follows: LAH > SDB > BCE > UNB. Higher PAH concentrations, especially in the water and sediment at LAH and SDB, are not surprising, insofar as both water bodies are heavily used for commercial and/or military shipping activities, and historical sediment contamination at these sites has been well documented [16,19]. In addition, both LAH and SDB are adjacent to heavily urbanized areas, with numerous potential PAH sources, including atmospheric emissions (e.g., heavy-duty truck traffic, industrial activities, congested roadways), stormwater runoff draining highly urbanized watersheds [1,6], and direct discharges (e.g., oil spills). Both UNB and BCE are also adjacent to urban areas, but neither site had the commercial/military shipping activities or heavy industrial activities that were associated with LAH and SDB. Concentrations in all media at UNB were at least one order of magnitude lower than at the other three sites. This was not surprising, insofar as UNB is the watershed with the lowest degree of urbanization and the greatest percentage of open space among the sample sites by far.

The concentration ranges of PAH observed in the present study were generally within the range of concentrations reported elsewhere for urban areas (Table 4). The highest air concentrations of PAH in southern California were approximately 20 to 40% lower than those in other highly urban coastal areas (San Francisco, Baltimore, New York–New Jersey), but dissolved water concentrations were nearly twice as high at LAH compared with Baltimore Harbor, seven times higher than those in San Francisco Estuary, and similar to those in New York Harbor. Sediment concentrations in the present study were generally within the range observed in these same urban harbors.

PAH distributions and sources

With few exceptions, the distributions of PAH compounds within the same medium were similar across sites, indicating a similar mix of sources within a given medium across the region. PAH distributions within the same medium were strongly correlated between LAH and SDB for both sediment and water column (both dissolved and on SPM; $r > 0.93$, $p < 0.001$). Moderate to strong correlations within the same medium were found across most sites for the atmosphere and the water column ($0.47 < r < 0.98$, $p < 0.01$). Exceptions included SDB and UNB, which were not significantly correlated ($p > 0.15$) with other sites in the atmospheric particle phase (SDB) and water column (UNB).

Table 3. Polycyclic aromatic hydrocarbon (PAH) concentrations in each medium by site (mean concentrations ± standard deviation are given where $n > 1$)

		Atmosphere		Water column		
Site[a]	Compound[b]	Gaseous (ng/m^3)	Particulate (ng/m^3)	Dissolved (ng/L)	SPM (ng/L)	Sediment (g dry wt)
BCE	*t*-PAH	15.5	1.71	10.6	19.2	2,460 ± 3,120
	2–3 ring PAH	8.6	0.41	5.1	14	360 ± 420
	4–6 ring PAH	6.9	1.3	5.5	5.2	2,100 ± 2,700
LAH	*t*-PAH	26 ± 9.4	2.06 ± 1.72	74 ± 15.1	72 ± 31	11,000 ± 1,280
	2–3 ring PAH	19 ± 5.5	0.36 ± 0.12	36 ± 7.7	28 ± 12	1,500 ± 180
	4–6 ring PAH	7.0 ± 3.9	1.7 ± 1.6	38 ± 7.4	44 ± 19	9,500 ± 1,100
UNB	*t*-PAH	3.3	0.263	5.6	3.3	657 ± 256
	2–3 ring PAH	2.2	0.053	2.9	1.9	77 ± 25
	4–6 ring PAH	1.1	0.21	2.7	1.4	580 ± 230
SDB	*t*-PAH	22	2.5	53 ± 4.8	44 ± 41.1	6,740 ± 536
	2–3 ring PAH	10	1.1	20 ± 3.5	31 ± 33	640 ± 76
	4–6 ring PAH	12	1.4	33 ± 1.3	13 ± 8.1	6,100 ± 460

[a] BCE = Ballona Creek Estuary, CA, USA; LAH = Los Angeles Harbor, CA, USA; UNB = Upper Newport Bay, CA, USA; SDB = San Diego Bay, CA, USA.
[b] *t*-PAH = sum of the 28 target PAH compounds listed in Table 2. SPM = suspended particulate matter.

Table 4. Comparison of total polycyclic aromatic hydrocarbon (*t*-PAH) concentrations in the atmopshere, water column, and sediment

	Southern California, USA[a]	San Francisco Estuary, CA, USA[b,c]	Baltimore Harbor, MD, USA[d,e,f]	New York/New Jersey Harbor, USA[g,h]
Atmosphere				
Gas phase (ng/m^3)	3.3–26	6.7–31	39	13–44
Particle phase (ng/m^3)	0.26–2.5		2.1	0.83–3.0
Water column				
Dissolved (ng/m^3)	5,600–74,000	6,633–10,859	44,820	10,677–72,183
Sediment (ng/g dry wt)	657–11,000	955–3,884	90–46,200	5,887

[a] This study; range of site means.
[b] Tsai et al. [42]; air *t*-PAH = 39, dissolved water *t*-PAH = 26.
[c] Pereira et al. [43]; sediment *t*-PAH = 21; data reported for 0–10 cm depth only.
[d] Dachs et al. [9]; air *t*-PAH = 24.
[e] Bamford et al. [11]; dissolved water *t*-PAH = 13.
[f] Ashley et al. [44]; sediment *t*-PAH = 32.
[g] Gigliotti et al. [12]; air/water *t*-PAH = 36.
[h] Lamoureux et al. [45]; sediment *t*-PAH = 26.

The distributions of PAH compounds across media within a given site were also similar, again linking these compartments and suggesting a similar mix of sources across media within a site. In all cases, the strongest correlations between PAH distributions across media were observed at LAH ($0.58 < r < 0.75$, $p < 0.001$). Moderate correlations were observed between PAH distributions in the atmospheric gas phase and the dissolved water column ($r > 0.49, p < 0.008$) except at SDB, and the dissolved water column and the sediment pore water ($0.411 < r < 0.72, p < 0.03$) at all sites. Moderate correlations were also observed between PAH distributions in the sediment and on SPM ($0.45 < r < 0.75, p < 0.02$) at all sites.

Differentiation between major source categories (pyrogenic vs petrogenic) was evaluated through characteristic diagnostic ratios (Fig. 2). With few exceptions, the diagnostic ratios used were indicative of predominantly pyrolytic sources (e.g., combustion) of PAH in the sediment and water column at most sites (anthracene/(anthracene + phenanthrene) > 0.1 and fluoranthene/(fluoranthene + pyrene) > 0.4) [40]. This is not surprising, in that the study sites are all located within/adjacent to large urban centers, with an abundance of both current and historical combustion emission sources of PAH, including atmospheric emissions and watershed sources (e.g., runoff). The exception was SDB, which had diagnostic ratios indicative of a mix of petrogenic and pyrolytic sources both in the sediment and on SPM. This suggests that, in addition to atmospheric and watershed sources of combustion-derived PAH, direct discharges of petroleum products, such as oil spills/leaks (which are not unexpected because of the large amount of shipping activities), likely contributed to PAH concentrations in the bay as well.

Exchange between the atmosphere and the water column

The net gas exchange flux (volatilization–absorption) was positive (net volatilization) at UNB, SDB, and LAH and

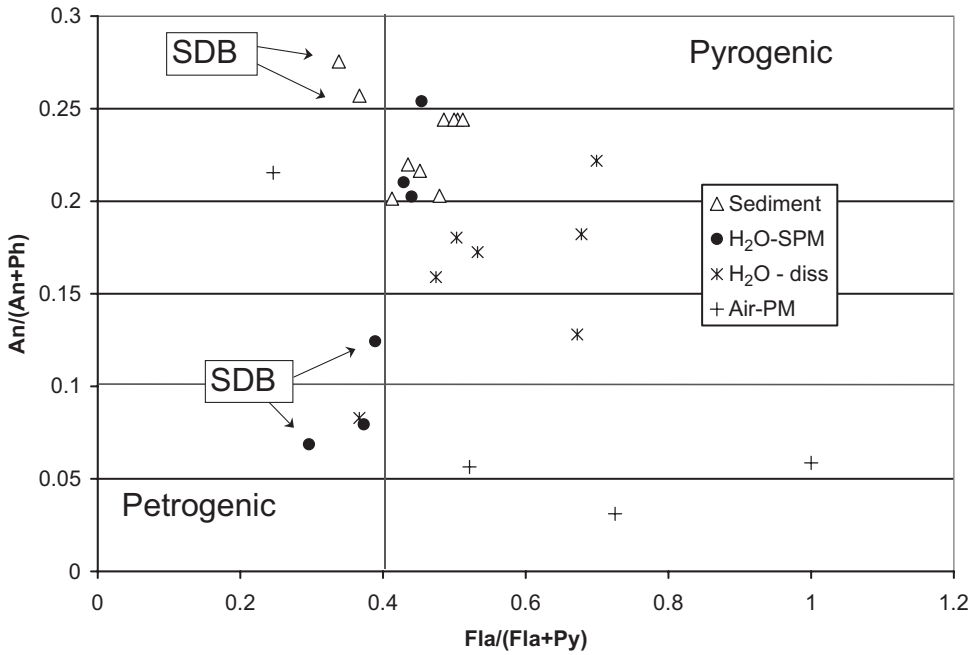

Fig. 2. Polycyclic aromatic hydrocarbon diagnostic ratios. Fla, fluoranthene; Py, pyrene; An, anthracene; Ph, phenanthrene. (Fla)/(Fla + Py) > 0.4 = pyrogenic, < 0.4 = petrogenic sources; An/(An + Ph) > 0.1 = pyrogenic, < 0.1 = petrogenic sources. SDB, San Diego Bay (CA, USA) site; SPM, suspended particulate matter.

Table 5. Estimated multimedia exchange fluxes of polycyclic aromatic hydrocarbons (PAH) in units of ng/m^2/day: A positive air–water flux indicates movement from the water to the atmosphere (upward); a positive sediment–water flux indicates movement from the sediment to the water (upward)

		Air–water exchange fluxes			Sediment–water exchange fluxes		
Site[a]	Compound[b]	Gas exchange	Dry particle deposition	Net air–water exchange	Diffusive exchange	Sedimentation	Net sediment–water exchange
BCE	*t*-PAH	−700	−270	−970	390,000	−15,000	375,000
	2–3 ring PAH	300	−70	230	300,000	−10,000	290,000
	4–6 ring PAH	−1,000	−200	−1,200	90,000	−5,000	85,000
LAH	*t*-PAH	7,000	−360	6,640	380,000	−70,000	310,000
	2–3 ring PAH	5,000	−60	4,940	300,000	−30,000	270,000
	4–6 ring PAH	2,000	−300	1,700	80,000	−40,000	40,000
UNB	*t*-PAH	295	−50	245	100,000	−3,000	97,000
	2–3 ring PAH	300	−10	290	80,000	−2,000	78,000
	4–6 ring PAH	−5	−40	−45	20,000	−1,000	19,000
SDB	*t*-PAH	4,800	−400	4,400	290,000	−40,000	250,000
	2–3 ring PAH	4,000	−200	3,800	200,000	−30,000	170,000
	4–6 ring PAH	800	−200	600	90,000	−10,000	80,000

[a] BCE = Ballona Creek Estuary, CA, USA; LAH = Los Angeles Harbor, CA, USA; UNB = Upper Newport Bay, CA, USA; SDB = San Diego Bay, CA, USA.
[b] *t*-PAH = sum of the 28 target PAH compounds listed in Table 2.

negative (net absorption) at BCE (Table 5). The largest gas exchange fluxes, observed at LAH and SDB, were driven by the high water concentrations of PAH at these sites. Net absorption was observed at BCE, because this site had relatively low water concentrations (five to seven times lower than those at SDB and LAH) but air concentrations that were within a factor of two of those at these other sites. Upper Newport Bay, which had the lowest air and water concentrations, also had the smallest magnitude of gas exchange.

Dry particle deposition fluxes were typically an order of magnitude lower than gas exchange (Table 5). The negative sign for dry particle deposition indicates movement downward, from the air to the water. Dry particle deposition fluxes at SDB, LAH, and BCE were all within a factor of two, whereas UNB flux was five to eight times smaller. Dry particle deposition was dominated by four- to six-ring PAH, which typically constituted the bulk of the atmospheric particle phase.

The total net exchange between the atmosphere and the water column (gas exchange + dry particle deposition) indicated net volatilization at LAH, UNB, and SDB and net absorption at BCE (Table 5). Gas exchange was the dominant process of transport between the air and water at all sites. The overall magnitude of the net air–water exchange was larger at LAH and SDB than at BCE by five to seven times and larger than UNB by at least an order of magnitude.

Sensitivity analysis

For gas exchange, variations in temperature (and subsequent temperature-dependent changes in K_h) and wind speed were assessed, to account for the range of these parameters typical for southern California coastal areas. Temperatures at the coast in southern California do not vary greatly over the year, with an average daily low temperature in the winter of approximately 10°C, to an average daily high in the summer of 25°C (NCDC, 2006; http://www.ncdc.noaa.gov/oa.ncdc.html). Bamford et al. [35] observed an average percentage change in K_h over this temperature range of ±50%. Daily wind speeds in coastal areas of southern California typically average between 2 and 4 m/s, and more than 90% of the daily mean wind speeds were between 1 and 5 m/s in 2006 (NCDC, 2006; http://www.ncdc.noaa.gov/oa.ncdc.html).

At the LAH and SDB sites, the direction of the net gas exchange did not change with variations in temperature (between 10 and 25°C) and subsequent variation of ±50% K_h or wind speed (between 1 and 5 m/s). Thus, we expect net volatilization at LAH and SDB throughout the majority of the year. In contrast, for wind speeds greater than 1 m/s, increasing the temperature resulted in a change to net volatilization at BCE. Similarly, at wind speeds less than 5 m/s, decreasing the temperature resulted in a change to net absorption at UNB.

These results demonstrate that the water column acts as a net source to the atmosphere at LAH and SDB because of high water concentrations at these sites, which overwhelm any sensitivity to changing meteorological conditions. In contrast, for BCE and UNB, the atmosphere may be a source or a sink at different times of the year, depending on the meteorological conditions. Net volatilization is favored with higher temperatures and higher wind speeds, whereas net absorption is favored at lower temperatures and lower wind speeds.

Exchange between the water column and sediment

Diffusive fluxes of *t*-PAH between the water column and sediment were positive at all sites, indicating movement from the sediment to the water (Table 5). Los Angeles Harbor, SDB, and BCE diffusive fluxes were three to four times greater than those at UNB. Diffusive flux out of the sediment was dominated by two- or three-ring PAH (70–80%) even though concentrations in the sediment were dominated by four- to six-ring PAH. The smaller K_{OC} for the lighter PAH favored rapid transport from the sediment to the water column.

Sedimentation fluxes were one order of magnitude smaller than diffusive fluxes at all sites (Table 5). Because sedimentation was small compared with diffusive flux, the direction of net exchange between the water column and the sediment (diffusive + sedimentation) was dominated by diffusive exchange and indicated net transport from sediment to water at all sites (Table 5).

Sensitivity analysis

Sediment pore-water concentrations were estimated from equilibrium partitioning based on literature K_{OC} values and sediment concentrations. Literature K_{OC} values for some compounds can vary by as much as 50% because of differences in methods of determining K_{OC} as well as differences in sorbing properties of the test soil carbon [41]. Sensitivity analysis using K_{OC} values of $\pm 50\%$ produced diffusive flux estimates with the same direction of exchange and within the same order of magnitude as the fluxes reported in Table 5.

Significance of air–water and sediment–water fluxes

The results from the present study are the first to estimate air–water exchange rates of PAH for coastal embayments of southern California and then to compare those rates with other exchange processes. In all cases, the magnitude of the diffusive flux of PAH out of the sediments and into the water column far exceeds input or output of PAH through air–water exchange processes. For example, the water area of the Port of Los Angeles (POLA) is approximately 13 km^2. Based on the air–water and sediment–water exchange fluxes estimated for LAH, the net sediment contribution of PAH to the water column of POLA is approximately 1,500 kg/year, whereas the net removal of PAH from the water column into the atmosphere through air–water exchange is approximately 32 kg/year. Thus, because of high sediment concentrations, input to the water column from the sediment far exceeds input/output from the water column resulting from air–water exchange. These results imply an additional removal mechanism from the water column, which is likely water movements associated with local coastal currents. Other potential input mechanisms not quantified in the present study include watershed sources (e.g., storm- and dry-weather runoff), and resuspension of contaminated sediment (and subsequent desorption of PAH from resuspended sediments). Estimates for loading rates of PAH from watershed sources to the target waterbodies are limited, but available data include stormwater runoff from the Los Angeles River watershed (located adjacent to LAH), ranging from 35 to 150 kg/year [6]. This suggests that watershed sources exceed direct atmospheric inputs but remain at least an order of magnitude less than sediment input at LAH. These results demonstrate the importance of contaminated sediments as a source of PAH to the water column in coastal waters of southern California.

There are a number of limitations to the exchange estimates calculated in the present study. First, the small sample size ($n < 5$) at each site limits the applicability of the exchange estimates to larger spatial and temporal scales. Second, atmospheric samples were collected at land-based sites from 30 m (SDB) to as much as 4 km (BCE) from water collection sites. To minimize this limitation, every effort was made to select sites that were downwind of their target waterbody and generally representative of the number and types of PAH sources at the waterbody. Third, there are uncertainties in a number of literature-derived input parameters (e.g., K_h, K_{OC}) in the exchange models used in this paper. Finally, the equilibrium-partitioning model used here to predict partitioning between the sediment and the pore water may overestimate pore-water concentrations [14].

Despite the limitations of the present study, the fluxes reported here provide a reasonable estimate of movement between compartments based on parameters that were easily quantified for the systems studied. In addition, these results provide previously unavailable gas exchange and dry atmospheric deposition flux estimates for southern California coastal water bodies. These order-of-magnitude estimates indicate that sediments remain a source of PAH to the water column and, at the most polluted sites, to the local/regional atmosphere via volatilization from the water column. Because of high sediment concentrations, input to the water column from the sediment far exceeds input/output from the water column resulting from air–water exchange, under the conditions studied here (e.g., quiescent, nonstormwater conditions). A larger number of samples and additional measurement parameters (e.g., resuspension fluxes) would be required to refine the exchange estimates from the present study.

Acknowledgement—We thank Chuck Katz, Mark Edson, and Hadrianna delos Santos of the United States Navy; William Bretz from the UCI Marsh Reserve; Mas Dojiri from the City of Los Angeles; and Philip Fine and Sumner Wilson from the South Coast Air Quality Management District for their cooperation. Also, we express our appreciation for the Southern California Coastal Water Research Project personnel Rachel McPherson and Sandy Nguyen for their assistance in collecting the field data.

REFERENCES

1. Zeng EY, Vista CL. 1997. Organic pollutants in the coastal environment off San Diego, California. 1. Source identification and assessment by compositional indices of polycyclic aromatic hydrocarbons. *Environ Toxicol Chem* 16:179–188.
2. Menzie CA, Hoeppner SS, Cura JJ, Freshman JS, LaFrey EN. 2002. Urban and suburban storm water runoff as a source of polycyclic aromatic hydrocarbons (PAHs) to Massachusetts estuarine and coastal environments. *Estuaries* 25:165–176.
3. Mai B, Qi S, Zeng E, Yang Q, Zhang G, Fu J, Sheng G, Peng P, Wang Z. 2003. Distribution of polycyclic aromatic hydrocarbons in the coastal region off Macao, China: Assessment of input sources and transport pathways using compositional analysis. *Environ Sci Technol* 37:4855–4863.
4. Hoffman EJ, Mills GL, Latimer JS, Quinn JG. 1984. Urban runoff as a source of polycyclic aromatic hydrocarbons to coastal waters. *Environ Sci Technol* 18:580–587.
5. Simcik MF, Eisenreich SJ, Golden KA, Liu S-P, Lipiatou E, Swackhamer DL, Long DT. 1996. Atmospheric loading of polycyclic aromatic hydrocarbons to Lake Michigan as recorded in the sediments. *Environ Sci Technol* 30:3039–3046.
6. Stein ED, Tiefenthaler LL, Schiff K. 2006. Watershed-based sources of polycyclic aromatic hydrocarbons in urban storm water. *Environ Toxicol Chem* 25:373–385.
7. Peng J, Maruya K, Schiff K, Tsukada D, Diehl DW, Lao W, Gan J, Zeng EY. 2007. Organochlorine pesticides and other trace organic contaminants in the Upper Newport Bay watershed. Technical Report 512. Southern California Coastal Water Research Project, Costa Mesa, CA, USA.
8. Hoff RM, Strachan WMJ, Sweet CW, Shackleton M, Bidleman TF, Brice KA, Burniston DA, Cussion S, Gatz DF, Harlin K, Schroeder WH. 1996. Atmospheric deposition of toxic chemicals to the Great Lakes: a review of data through 1994. *Atmos Environ* 30:3505–3527.
9. Dachs J, Glenn TRI, Gigliotti CL, Brunciak PA, Totten LA, Nelson ED, Franz TP, Eisenreich SJ. 2002. Processes driving the short-term variability of polycyclic aromatic hydrocarbons in the Baltimore and northern Chesapeake Bay atmosphere, USA. *Atmos Environ* 36:2281–2295.
10. Franz TP, Eisenreich SJ, Holsen TM. 1998. Dry deposition of particulate polychlorinated biphenyls and polycyclic aromatic hydrocarbons to Lake Michigan. *Environ Sci Technol* 32:3681–3688.
11. Bamford HA, Offenberg JH, Larsen RK, Ko FC, Baker JE. 1999. Diffusive exchange of polycyclic aromatic hydrocarbons across the

air–water interface of the Patapsco River, an urbanized subestuary of the Chesapeake Bay. *Environ Sci Technol* 33:2138–2144.
12. Gigliotti CL, Brunciak PA, Dachs J, Glenn TRI, Nelson ED, Totten LA, Eisenreich SJ. 2002. Air–water exchange of polycyclic aromatic hydrocarbons in the New York–New Jersey, USA, harbor estuary. *Environ Toxicol Chem* 21:235–244.
13. Gschwend PM, Hites RA. 1981. Fluxes of polycyclic aromatic hydrocarbons to marine and lacustrine sediments in the northeastern United States. *Geochim Cosmochim Acta* 45:2359–2367.
14. McGroddy SE, Farrington JW. 1995. Sediment porewater partitioning of polycyclic aromatic hydrocarbons in three cores from Boston Harbor, Massachusetts. *Environ Sci Technol* 29:1542–1550.
15. Maruya K, Risebrough RW, Horne AJ. 1996. Partitioning of polynuclear aromatic hydrocarbons between sediments from San Francisco Bay and their porewaters. *Environ Sci Technol* 30:2942–2947.
16. Fairey R, Roberts C, Jacobi M, Lamerdin S, Clark R, Downing J, Long E, Hunt J, Anderson B, Newman J, Tjeerdema R, Stephenson M, Wilson C. 1998. Assessment of sediment toxicity and chemical concentrations in the San Diego Bay region, California, USA. *Environ Toxicol Chem* 17:1570–1581.
17. Latimer JS, Davis WR, Keith DJ. 1999. Mobilization of PAHs and PCBs from in-place contaminated marine sediments during simulated resuspension events. *Estuar Coast Shelf Sci* 49:577–595.
18. Mitra S, Dellapenna TM, Dickhut RM. 1999. Polycyclic aromatic hydrocarbon distribution within lower Hudson River estuarine sediments: physical mixing vs sediment geochemistry. *Estuar Coast Shelf Sci* 49:311–326.
19. Anderson BS, Hunt JW, Phillips BM, Fairey R, Roberts CA, Oakden JM, Puckett HM, Stephenson M, Tjeerdema RS, Long ER, Wilson CJ, Lyons JM. 2001. Sediment quality in Los Angeles Harbor, USA: A triad assessment. *Environ Toxicol Chem* 20:359–370.
20. Wang X-C, Zhang Y-X, Chen RF. 2001. Distribution and partitioning of polycyclic aromatic hydrocarbons (PAHs) in different size fractions in sediments from Boston Harbor United States. *Mar Pollut Bull* 42:1139–1149.
21. Bay SM, Zeng EY, Lorenson TD, Tran K, Alexander C. 2003. Temporal and spatial distributions of contaminants in sediments of Santa Monica Bay, California. *Mar Environ Res* 56:255–276.
22. Lohmann R, Macfarlane JK, Gschwend PM. 2005. Importance of black carbon to sorption of native PAHs, PCBs, and PCDDs in Boston and New York Harbor sediments. *Environ Sci Technol* 39:141–148.
23. Maruya KA, Schiff K. 2009. The extent and magnitude of sediment contamination in the Southern California Bight. In Lee HJ, Normark WR, eds, *Earth Science in the Urban Ocean: The Southern California Continental Borderland*. Geological Society of America Special Paper 454. Geological Society of America, Boulder, CO, pp 399–412.
24. State Water Resources Control Board. 2003. Approval of the 2002 Federal Clean Water Act Section 303(d) list of Water Quality Limited Segments. Resolution 2003-0009. Sacramento, CA, USA.
25. Zeng E, Yu CC, Tran K. 1999. In situ measurements of chlorinated hydrocarbons in the water column off the Palos Verdes Peninsula, California. *Environ Sci Technol* 33:392–398.
26. Whitman WG. 1923. The two film theory of gas absorption. *Chem Metal Engineer* 29:146–148.
27. Liss PS, Slater PG. 1974. Flux of gases across the air–sea interface. *Nature* 247:181–184.
28. Schwarzenbach RP, Gschwend PM, Imboden DM. 1993. *Environmental Organic Chemistry*. John Wiley & Sons, New York, NY, USA.
29. Wanninkhoff R. 1992. Relationship between windspeed and gas exchange over the ocean. *J Geophys Res* 97:7373–7382.
30. Achman DR, Hornbuckle KC, Eisenreich SJ. 1993. Volatilization of polychlorinated biphenyls from Green Bay, Lake Michigan. *Environ Sci Technol* 27:75–87.
31. Eisenreich SJ, Hornbuckle KC, Achman DR. 1997. Air–water exchange of semivolatile organic chemicals in the Great Lakes. In Baker JE, ed, *Atmospheric Deposition of Contaminants to the Great Lakes and Coastal Waters*. SETAC, Pensacola, FL, USA, pp 109–135.
32. Totten LA, Brunciak PA, Gigliotti CL, Dachs J, Glenn TRI, Nelson ED, Eisenreich SJ. 2001. Dynamic air–water exchange of polychlorinated biphenyls in the New York–New Jersey Harbor Estuary. *Environ Sci Technol* 35:3834–3840.
33. Fuller EN, Schettler PD, Giddings JC. 1966. A new method for prediction of binary gas-phase diffusion coefficients. *Indust Engineer Chem* 58:19–27.
34. Wilke CR, Chang P. 1955. Correlation of diffusion coefficients in dilute solutions. *Am Inst Chem Engineer J* 1:264–270.
35. Bamford HA, Poster DL, Baker JE. 1999. Temperature dependence of Henry's Law constants of thirteen polycyclic aromatic hydrocarbons between 4°C and 31°C. *Environ Toxicol Chem* 18:1905–1912.
36. Mackay D, Shiu W-Y, Ma K-C. 1999. *Physical–Chemical Properties and Environmental Fate and Degradation Handbook*. CRC, Boca Raton, FL, USA.
37. Delle Site A. 2001. Factors affecting sorption of organic compounds in natural sorbent/water systems and sorption coefficients for selected pollutants. A review. *J Phys Chem Ref Data* 30:187–439.
38. Mackay D, Shiu W-Y, Ching MK. 1992. *Illustrated Handbook of Physical–Chemical Properties and Environmental Fate for Organic Chemicals*, Vol II—*Polynuclear Aromatic Hydrocarbons, Polychlorinated Dioxins, and Dibenzofurans*. Lewis, Boca Raton, FL, USA.
39. Mackay D. 2001. *Multimedia Environmental Models: The Fugacity Approach* 2nd ed. CRC, Boca Raton, FL, USA.
40. Yunker MB, Macdonald RW, Vingarzan R, Mitchell RH, Goyette D, Sylvestre S. 2002. PAHs in the Fraser River basin: a critical appraisal of PAH ratios as indicators of PAH source and composition. *Org Geochem* 33:489–515.
41. Karickhoff SW, Brown DW, Scott TA. 1979. Sorption of hydrophobic pollutants on natural sediments. *Water Res* 13:214–248.
42. Tsai P, Hoenicke R, Yee D, Baker JE, Bamford HA. 2005. San Francisco Bay Atmospheric Deposition Pilot Study Part 3: Dry Deposition of PAHs and PCBs. Final Report 408. San Francisco Estuary Institute, Oakland, CA, USA.
43. Pereira WE, Hostettler FD, Luoma SN, van Green A, Fuller CC, Anima RJ. 1999. Sedimentary record of anthropogenic and biogenic polycyclic aromatic hydrocarbons in San Francisco Bay, California. *Mar Chem* 64:99–113.
44. Ashley JTF, Baker JE. 1999. Hydrophobic organic contaminants in surficial sediments of Baltimore Harbor: Inventories and sources. *Environ Toxicol Chem* 18:838–849.
45. Lamoureux EM, Brownawell BJ. 1999. Chemical and biological availability of sediment-sorbed hydrophobic organic contaminants. *Environ Toxicol Chem* 18:1733–1741.